Structural analysis for shallow tunnels in soft soils

Vu Minh, N.; Broere, Wout; Bosch, Johan W.

DOI
10.1061/(ASCE)GM.1943-5622.0000866

Publication date
2017

Document Version
Final published version

Published in
International Journal of Geomechanics

Structural Analysis for Shallow Tunnels in Soft Soils

Minh Ngan Vu[1]; Wout Broere[2]; and Johan W. Bosch[3]

Abstract: Generally, studies on structural design for bored tunnels focus on moderate to deep tunnels (cover-to-diameter ratio $C/D \geq 2$). Such tunnel design methods cannot be used for shallow-situated bored tunnels because the influence of buoyancy is discounted, and actual loads on the tunnel lining are not taken into account properly. This paper proposes a new model that has more accurate loads on the tunnel lining combined with finite-element analysis for shallow tunnels. Internal forces and deformations of various shallow bored tunnels are investigated. The relationship between the optimal thickness-to-diameter ratio d/D of the tunnel cross section and the cover-to-diameter ratio C/D is also studied. **DOI: 10.1061/(ASCE)GM.1943-5622.0000866.**

Author keywords: Cover-to-diameter ratio; Tunnel lining; Shallow bored tunnel; Soft soil.

Introduction

Tunnel boring machines are widely used in the construction of underground infrastructures in urban areas because disturbances at the surface level can be reduced significantly during the construction and because of their ability to limit settlements and damage to existing buildings. In an environment with soft overburden, particularly in soft Holocene layers, buildings are generally built on pile foundations. The tunnel is often designed well below the pile tip level. This is done for two reasons: to decrease interaction between the tunneling process and the piles, and to avoid having to drive through old abandoned piles that are still present below the streets. This results in relatively deep track tunnels and in deep station boxes. If the tunnels could be located at more shallow levels, such that they are located above the pile toe level, then the impact of tunneling-induced soil displacements would be largely eliminated. Such a reduction of the tunnel depth would also reduce the required depth of the station boxes and the construction costs. Other advantages are the low operational expenditure in the long-term and the shorter traveling time between the surface and the platforms.

Taking into account these conditions, this paper takes a look at the structural design of tunnel linings for shallow tunnels in soft soils. Many calculation models have been proposed and developed since 1926 for tunnel design. Schmid (1926) proposed the first analysis method for an elastic continuum. Schulze and Duddeck (1964) presented a bedded ring model for shallow tunnels with limited cover. Morgan (1961) proposed an analytical solution using continuum models, which takes into account the elliptical deformation of the tunnel lining. Windels (1966) further improved the method of Schulze and Duddeck (1964) by taking into account the second order of the series expansion of the analytical solution and the displacement of the tunnel lining in the construction process. Windels (1967) published a model for a circular tunnel in an elastic continuum with geometrical nonlinearity. Muir Wood (1975) corrected Morgan (1961) by including the tangential stresses on the model, but the radial deformations due to these stresses were ignored. This problem was then solved by Muir Wood (1976).

The common method used in practical tunnel design was proposed by Duddeck and Erdmann (1985). A continuum model and a bedded-beam model without a reduction of ground pressure at the crown are proposed for shallow tunnels with a ratio $C/D \leq 2$. The continuum model includes the interaction between soil and structure automatically. In the bedded-beam model, the interaction between soil and structure is captured by bedding springs with suitable applied stiffness. Duddeck (1988) indicated that the bedded-beam model or an equivalent continuum model may be suitable for calculating the internal forces in a shallow tunnel in soft soils. Blom (2002) included the effects of longitudinal joints and soil reactions to estimate the deformation of the tunnel lining.

Based on the models of Duddeck and Erdmann (1985), Oreste (2007) proposed a hyperstatic reaction method to estimate the internal forces in the tunnel lining by using a FEM framework for the tunnel in rock. Although this model simulates interactions between tunnel lining and surrounding ground through Winkler springs, only radial pressures are taken into account. A further developed model presented by Do et al. (2014) includes the tangential pressures. This model also takes into account the influence of segmental joints, which is indicated in Groeneweg (2007).

Although many models have been studied and developed, most of them focus on moderate and deep tunnels ($C/D \geq 2$). For shallow tunnels, especially very shallow tunnels that have a C/D ratio from 0 to 0.5, there has been little research. This paper looks into the effects of overburden on internal forces and deformations of the tunnel lining and seeks the optimal C/D ratio when tunneling in soft (Holocene) layers.

Structural Lining Design

When designing a tunnel in soft soils, the following assumptions are applied in most common design models (Duddeck and Erdmann 1985):

1. The stress-strain deformations of a cross section are in plane strain conditions for both the tunnel lining and the ground.

[1]Researcher, Geo-Engineering Section, Delft Univ. of Technology, Stevinweg 1, 2628 CN, Delft, Netherlands (corresponding author). E-mail: N.Vuminh@tudelft.nl

[2]Assistant Professor, Geo-Engineering Section, Delft Univ. of Technology, Stevinweg 1, 2628 CN, Delft, Netherlands. E-mail: W.Broere@tudelft.nl

[3]Professor, Geo-Engineering Section, Delft Univ. of Technology, Stevinweg 1, 2628 CN, Delft, Netherlands. E-mail: J.W.Bosch@tudelft.nl

Note. This manuscript was submitted on April 5, 2016; approved on October 24, 2016; published online on March 29, 2017. Discussion period open until August 29, 2017; separate discussions must be submitted for individual papers. This paper is part of the ***International Journal of Geomechanics***, © ASCE, ISSN 1532-3641.

2. The active soil pressures on the tunnel lining are equal to the primary stresses in the undisturbed ground before tunneling.
3. At the final stage of tunneling and in the long-term period, the ground will return to the conditions prior to tunneling.
4. The interaction between ground and tunnel lining is limited to radial and tangential or only radial springs.
5. Ground and tunnel lining are elastic materials.

These assumptions are also applied to the proposed model in this paper.

Influence of Load and Overburden on Lining Models

For the shallow tunnel, according to Duddeck (1988), a continuum model or a bedded-beam model without a reduction of ground pressure at the crown should be used in the design. Most of the models in the studies of Muir Wood (1975), Einstein and Schwartz (1979), Duddeck and Erdmann (1985), Möller (2006), Plizzari and Tiberti (2006), and Do et al. (2014) use a uniform load of vertical pressure on the tunnel lining at upper and lower parts of the tunnel, which is equal to the overburden pressure as

$$\sigma_v = \gamma H \tag{1}$$

where γ = volumetric weight of soil; and H = depth of the tunnel (at spring line location).

The horizontal pressure on the sides of the tunnel is constant and is given by

$$\sigma_h = K\sigma_v \tag{2}$$

where K = coefficient of horizontal effective stress at rest.

In shallow tunnels with a C/D ratio less than 2, the overburden pressure on the crown and the bottom tunnel parts is significantly different. The loading used in Duddeck's methods (Duddeck and Erdmann 1985), therefore, is not applicable in the case of shallow tunnels. To be more accurate, in this study, the vertical pressures should be calculated at every particular point of the tunnel cross section.

In the new model proposed in Fig. 1 for a shallow tunnel with radius R at the depth H, the vertical soil pressure on the tunnel lining σ_v can be estimated as

$$\sigma_v = \gamma(H + R\cos\theta) \tag{3}$$

where θ = angle between the element axis and the vertical axis of a tunnel section.

The horizontal soil pressure on the tunnel lining σ_h is given by

$$\sigma_h = K\gamma(H + R\cos\theta) \tag{4}$$

Unlike the methods of Duddeck and Erdmann (1985) and Blom (2002) for the reduction of vertical pressures at the lower part of the tunnel, the previously mentioned assumptions indicate that the active soil pressures on the tunnel lining are equal to the primary stresses in the undisturbed ground before tunneling. Therefore, there is no reduction of vertical pressures in the case of a shallow tunnel in this model.

Influence of Ground-Tunnel Lining Interaction

The interaction between soil and the tunnel lining is presented via the spring stiffness in this model. According to the hypothesis of Winkler (1867), the spring stiffness is estimated as

$$p = kS \tag{5}$$

where p = ground reaction pressure; S = radial displacement of the tunnel lining; and k = ground reaction modulus.

In Duddeck's bedded-beam models (Duddeck and Erdmann 1985), the stiffness of radial spring k_r is given by

$$k_r = E_s/R \tag{6}$$

where the stiffness modulus of the ground E_s is estimated as

$$E_s = E_c(1-\nu)/[(1+\nu)(1-2\nu)] \tag{7}$$

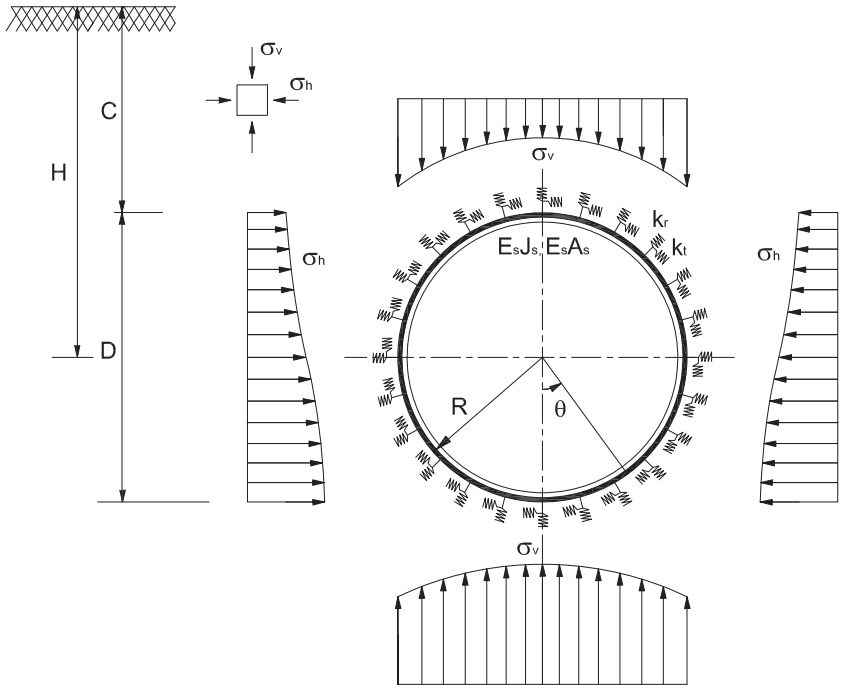

Fig. 1. Soil pressures on the tunnel lining

where E_c = elasticity modulus of the ground; and ν = Poisson's ratio.

These methods use a constant spring stiffness for every point on the tunnel lining based on the stiffness modulus of the ground and Poisson's ratio ν. This is not appropriate because the spring stiffness of each point on the tunnel lining is different due to the stress state of the soil and the change of the deformation pattern of the tunnel lining.

Oreste (2007) and Do et al. (2014) use a nonlinear relationship between the reaction pressure of the ground p and the deformation of the tunnel lining δ in Duddeck's model (Duddeck and Erdmann 1985) to calculate internal forces in the tunnel lining. The apparent stiffness of the ground η^* is estimated as

$$\eta^* = \frac{p_{\text{lim}}}{\delta}\left(1 - \frac{p_{\text{lim}}}{p_{\text{lim}} + \eta_0 \delta}\right) \tag{8}$$

where p_{lim} = maximum reaction pressure that the ground can offer; and η_0 = initial stiffness of the ground (for the δ value close to 0).

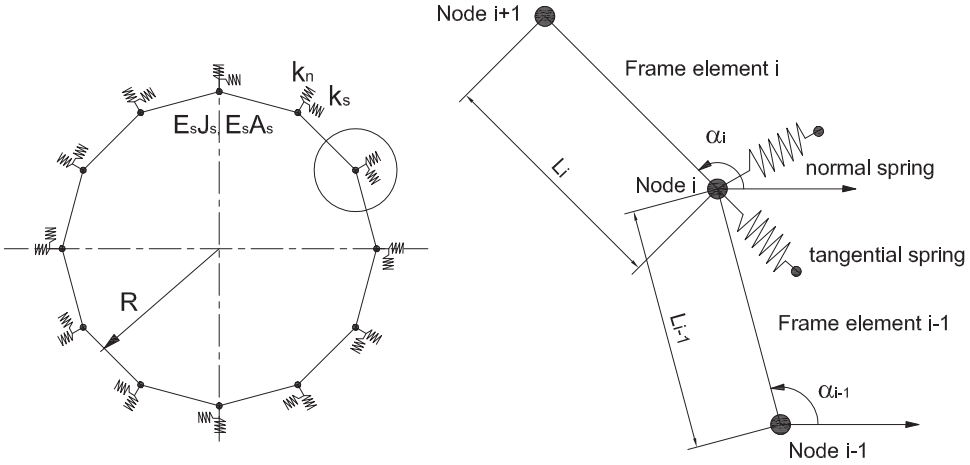

Fig. 2. Radial and tangential Winkler springs in FEM analysis (adapted from Do et al. 2014)

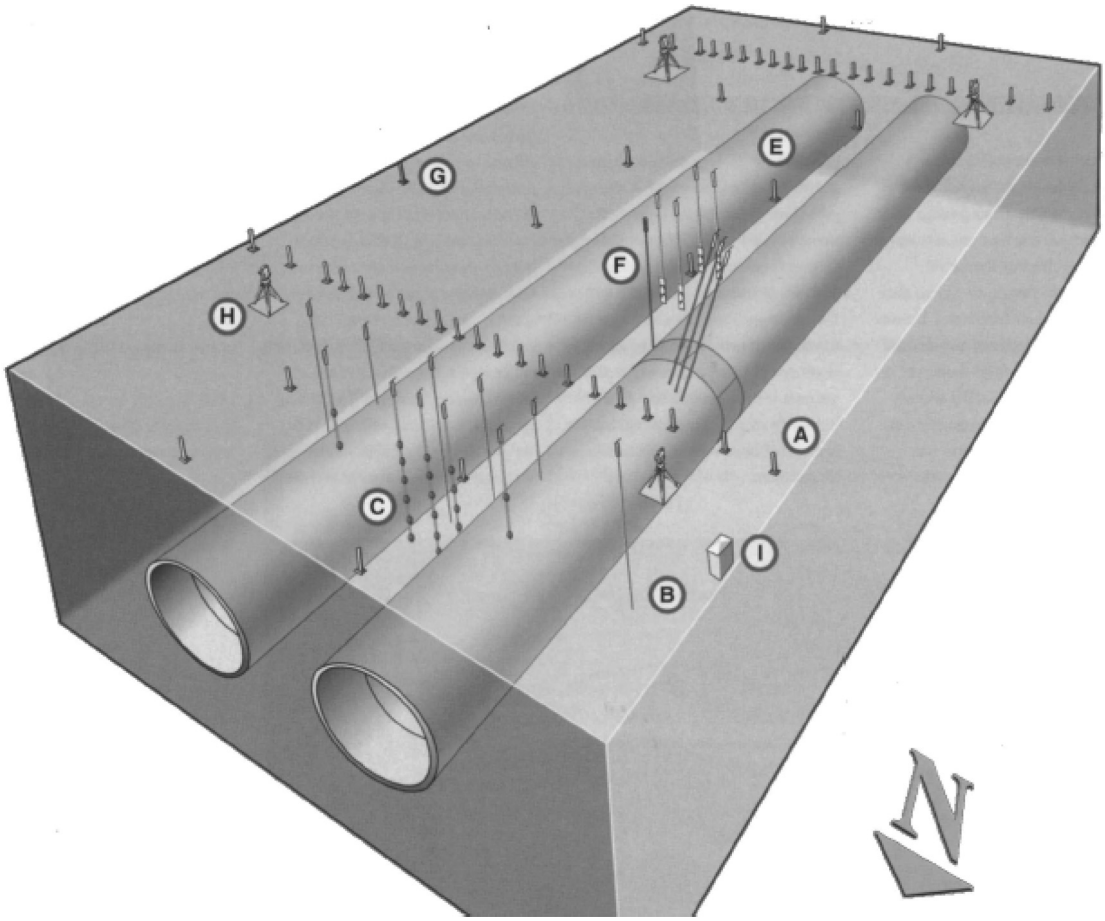

Fig. 3. Measuring field at Second Heinenoord Tunnel (reprinted from Broere 2001, with permission)

Table 1. Description of Layers and Soil Parameters for the North Bank of the Second Heinenoord Tunnel (Data from Bakker 2000)

Symbol	Soil type	Top of layer (m) N.A.P.	Unit weight, γ_{wet} (γ_{dry}) (kN/m^3)	Undrained shear strength, c_u (kPa)	Cohesion, c (kPa)	Friction angle, φ' (degrees)	Poisson's ratio, ν (–)	Elastic modulus, E (MPa)	Earth pressure coefficient, K_0 (–)
$OA + OB + 1$	Mixture of sand and clay	+2.50	17.2 (16.5)	—	3	27	0.34	5.2	0.58
3	Sand, local parts of clay	−1.50	19.5	—	0	35	0.3	26	0.47
2	Sand with clay	0–5.75	19	—	0	33	0.31	25	0.47
18	Sand, local parts of clay	−10.00	20.5	—	0	36.5	0.3	40	0.45
32	Sand, gravel	−17.25	20.5	—	0	36.5	0.3	60	0.5
38A	Clay, local parts of sand	−20.75	20.0	140	7	31	0.32	16	0.55
38F	Sand	−25	21	—	0	37.5	0.3	80	0.55
38A	Clay, local parts of sand	−26.5	20.0	140	7	31	0.32	16	0.55

Note: OA, OB = man-made fills; N.A.P. = Nieuw Amsterdam Peil (Dutch reference level, approx. mean sea level).

For a circular tunnel in elastic ground, the interaction between ground and the tunnel lining depends on the radius R of the tunnel lining and the ground parameters. The initial radial ground reaction stiffness $\eta_{r,0}$ is estimated as the following empirical formula (Möller 2006):

$$\eta_{r,0} = \beta \frac{1}{1+\nu}\frac{E}{R} \tag{9}$$

where E = Young's modulus of the ground; and β = dimensionless factor.

The value of β depends on soil and structural parameters, therefore, it is difficult to determine the exact β value. In conventional studies of Mashimo and Ishimura (2005), Möller (2006), Plizzari and Tiberti (2006), and Molins and Arnau (2011), the value of β is taken equal to 1. In Do et al. (2014), the value of β is taken equal to 2 compared with the Einstein and Schwart's (1979) method. In this study, the value of $\beta = 2$ is used in the analysis to determine the impact of the depth of cover on internal forces and deformations of the tunnel lining.

According to Mashimo and Ishimura (2005), Möller (2006), Plizzari and Tiberti (2006), and Molins and Arnau (2011), the simple relationship between tangential spring stiffness η_s and normal spring stiffness η_r is

$$\eta_s = \frac{1}{3}\eta_n \tag{10}$$

The maximum radial reaction pressure $p_{n,\lim}$ in Eq. (8) can be calculated as

$$p_{n,\lim} = \frac{2c\cos\varphi}{1-\sin\varphi} + \frac{1+\sin\varphi}{1-\sin\varphi}\Delta\sigma_{conf} \tag{11}$$

where c = cohesion; φ = friction angle; and $\Delta\sigma_{conf}$ = confining pressure on the tunnel perimeter estimated as

$$\Delta\sigma_{conf} = \frac{\sigma_h + \sigma_v}{2}\frac{\nu}{1-\nu} \tag{12}$$

Similar to Do et al. (2014), the maximum shear reaction pressure on the tunnel lining in Eq. (8) can be estimated as

$$p_{s,\lim} = \frac{\sigma_h + \sigma_v}{2}\tan\varphi \tag{13}$$

The stiffness of the radial springs $k_{n,i}$ and tangential springs $k_{s,i}$ in each element of the frame is

$$k_{n,i} = \eta^*_{n,i}\left[\frac{L_{i-1}+L_i}{2}\right] = \frac{p_{n,\lim}}{\delta_{n,i}}\left(1 - \frac{p_{n,\lim}}{p_{n,\lim} + \eta_{n,0}\delta_{n,i}}\right)\frac{L_{i-1}+L_i}{2} \tag{14}$$

$$k_{s,i} = \eta^*_{s,i}\left[\frac{L_{i-1}+L_i}{2}\right] = \frac{p_{s,\lim}}{\delta_{s,i}}\left(1 - \frac{p_{s,\lim}}{p_{s,\lim} + \eta_{s,0}\delta_{s,i}}\right)\frac{L_{i-1}+L_i}{2} \tag{15}$$

where L_i = distance between node ith and node $(i+1)th$ (Fig. 2). The values of $p_{n,\lim}$ and $p_{s,\lim}$ are estimated as Eqs. (11)–(13) for each integration element of the tunnel lining (here 360 elements of 1° segment) as detailed in Do et al. (2014).

The radial springs are only active in the compression condition. It means that in the area in which the tunnel moves away from the soil the radial springs are inactive.

Case Study of Second Heinenoord Tunnel

The validation of the new model is performed with the case study of the Second Heinenoord Tunnel in the Netherlands. A tunnel with an outer diameter of 8.3 m was constructed below the Oude Maas river in Rotterdam between 1996 and 1999. In this project there were two measurement locations, one on the North Bank and one on the South Bank. The layout of the measurement field at the North Bank is shown in Fig. 3. Measurement instruments were installed in all seven elements of a ring to derive the stress distribution in the ring. Pressure cells were installed on the outer face of segments with two cells per segment on seven segments. During the construction, bending moments and normal forces in the lining were measured using strain gauges.

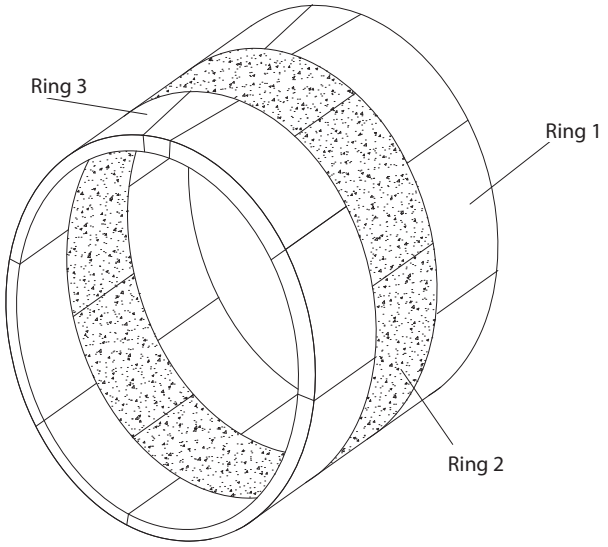

Fig. 4. A 3D model of segmental lining in *ANSYS* FEM analysis in Bakker et al. (2000)

On the North Bank, the tunnel axis is located at about 16.25 m below the surface. With a tunnel diameter of 8.3 m, the *C*/*D* ratio at this location is approximately 2. The description of soil layers and soil parameters are shown in Table 1.

A back-analysis with two-dimensional (2D) FEM *PLAXIS* was performed as indicated in Bakker (2003). The soil properties used were $K = 0.5$ and $\gamma = 18$ kN/m^3, and the tunnel is located at $C/D = 2$ with a lining thickness $d = 0.35$ m. The derived bending moments and normal forces from the *PLAXIS* model were compared with the measured data in the North Bank. Moreover, a three-dimensional (3D) model with *ANSYS* FEM software (Fig. 4) was also analyzed to derive bending moments in the tunnel lining in this case (Bakker et al. 2000). In this analysis, the concrete segments were modeled as solid volume segments. Three rings were modeled using 8,100 elements. In this model, the interaction between the tunnel lining and the surrounding ground was modeled as linear springs in the radial direction, as in Duddeck and Erdmann (1985), with 1,418 spring elements in total. The bending moments were derived with three rings and were compared with the field data.

To validate the new model, calculations for the Second Heinenoord case have been made to derive internal forces in the

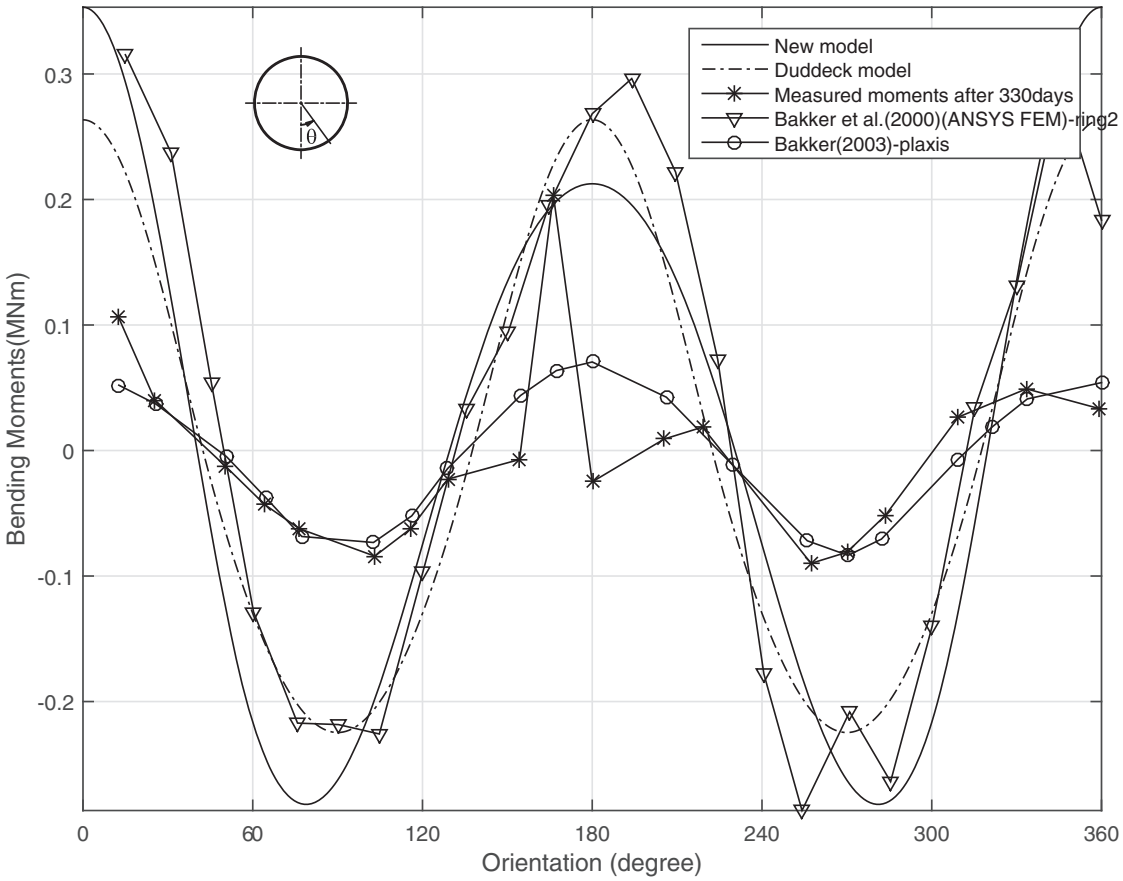

Fig. 5. Validation of bending moments in Second Heinenoord Tunnel

lining. The derived bending moments and normal forces from the new model are compared with the field data after 330 days and the analytical results from Bakker et al. (2000), as shown in Figs. 5 and 6.

A comparison among the bending moments derived from the new model and the bending moments from measurements in this project, Duddeck's bedded-beam model (Duddeck and Erdmann 1985), 2D *PLAXIS* model, and the 3D *ANSYS* model from Bakker et al. (2000) is shown in Fig. 5. This figure shows that bending moments derived from these models have the same bending moment trend as the measured data in the field. The bending moment derived from the new model is close to the moments derived from Duddeck's model and Bakker's 3D analysis by *ANSYS*. In comparison with the field data, the highest bending moment observed in the field data is close to the bending moments in all these models (at the location of 166° on the cross section of the tunnel lining). Even though there exists a difference between the measured bending moment at the sides of the tunnel lining, the highest bending moment at the top and the bottom of the tunnel lining shows an agreement between the field data and the analytical models.

Fig. 6 shows a comparison of normal forces between field data and normal forces derived from Duddeck's model (Duddeck and Erdmann 1985), Bakker's 2D *PLAXIS* model (Bakker et al. 2000), and the new model. Overall, normal forces calculated from these models have the same trend with measured normal forces in field data. From this figure, it can be seen that the normal force from the new model is closer to the field data than the results from Duddeck's model and Bakker's 2D *PLAXIS* model, especially at locations at the sides of the tunnel lining, although there still exists a difference between the analytical results and measured normal forces. It was explained in Bakker (2003) that the accuracy of the soil pressure gauges on the segments was unclear, and the influence of the grout injection pressure was not taken into account at the measured time of 330 days. This might also explain the strong variability in the measurement.

On the basis of this analysis, it is shown that the results derived from the new model have the same trend as the analysis results from previous numerical models and have a better agreement with the field data. In this case study with $C/D = 2$, the difference between these models is not very large, but for tunnels at shallower locations, the differences are expected to be larger. Unfortunately, detailed field measurements at the shallow overburden are lacking.

Comparing the Impacts of Overburden on the Tunnel Lining

Structural analysis is performed with Duddeck's bedded-beam model and the new model with and without buoyancy conditions in the model, as can be seen in Fig. 1. A circular tunnel with radius $D = 6.3$ m in soil condition with parameters $K = 0.5$, $\nu = 0.2$, $\gamma = 20$ kN/m^3, and $E = 20{,}000$ kN/m^2 has been analyzed and compared with the results in Duddeck and Erdmann (1985).

When comparing the internal forces derived from other methods of Ahrens et al. (1982), Windels (1967), Muir Wood (1976), and Einstein and Schwartz (1979), Duddeck and Erdmann (1985) used the following relative stiffness to investigate the effect of soil properties on the internal forces in the tunnel lining:

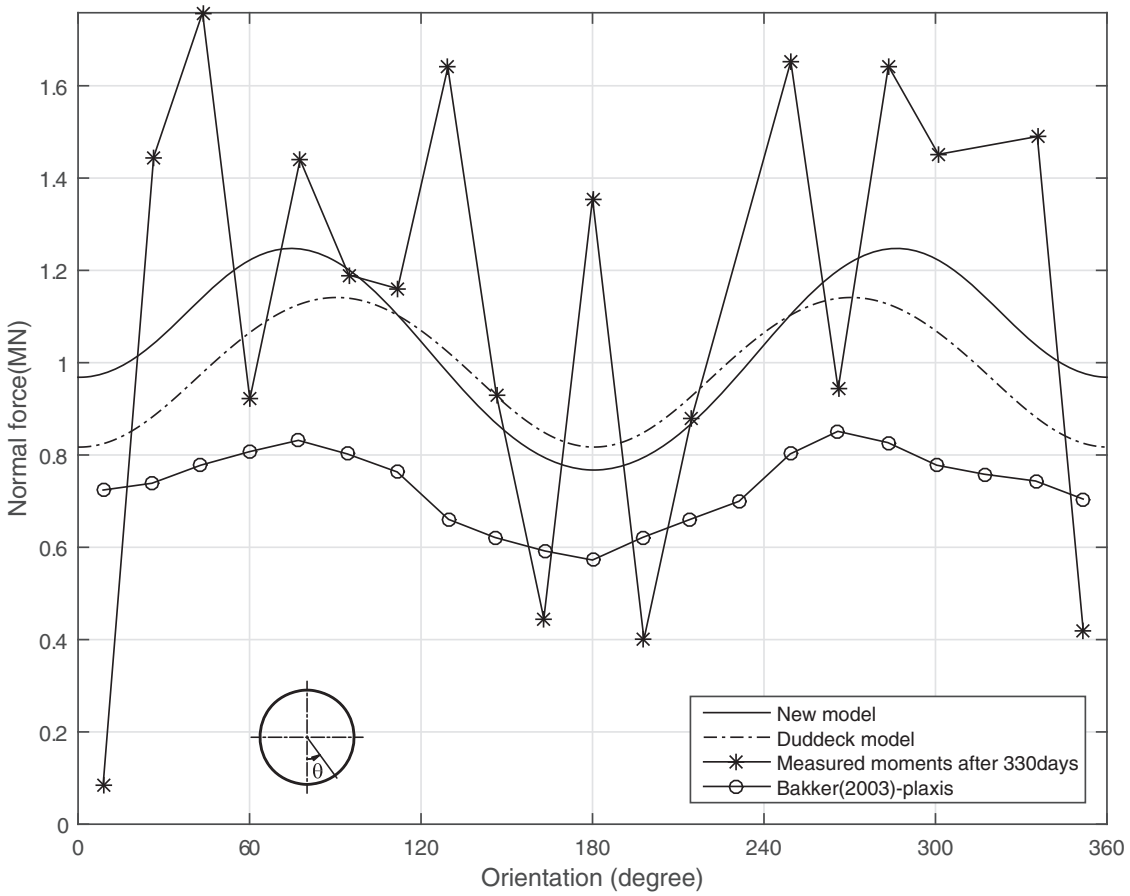

Fig. 6. Validation of normal forces in Second Heinenoord Tunnel

Int. J. Geomech., 2017, 17(8): 04017038

$$\alpha_D = \frac{ER^3}{E_l I_l} \tag{16}$$

where $E_l I_l$ = bending stiffness of the tunnel lining. This relative stiffness is also used in analysis results from the new model and Duddeck's model (Duddeck and Erdmann 1985).

In Figs. 7 and 8, the maximum bending moments M are calculated for a range of values of the relative stiffness α_D and plotted normalized to m, with m defined as

$$\max M = m\sigma_v R^2 \tag{17}$$

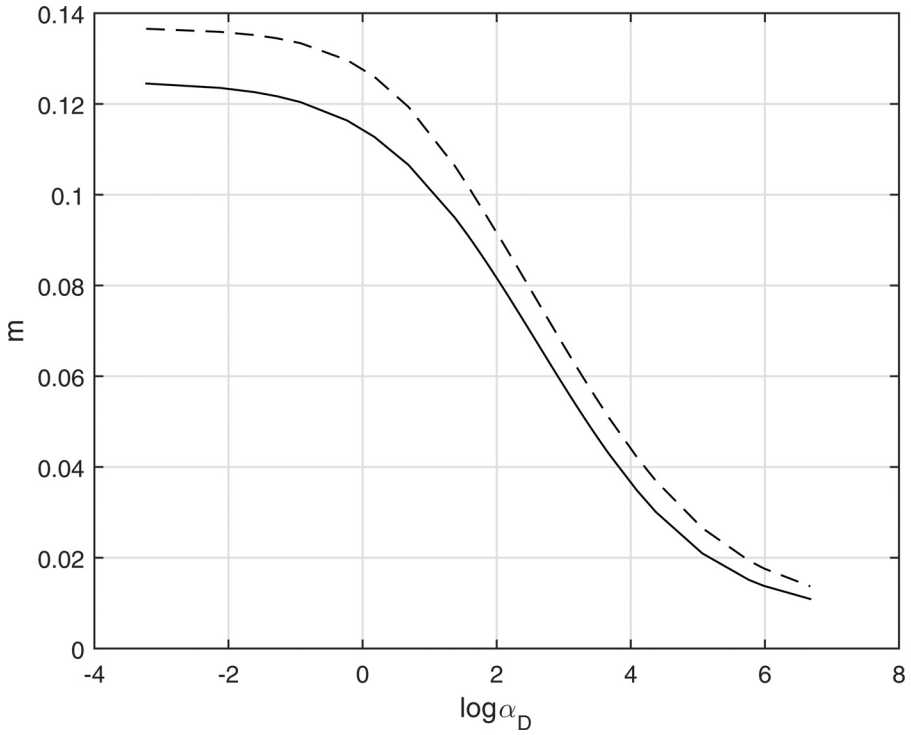

Fig. 7. Normalized maximum bending moments in models with various relative stiffness α_D values

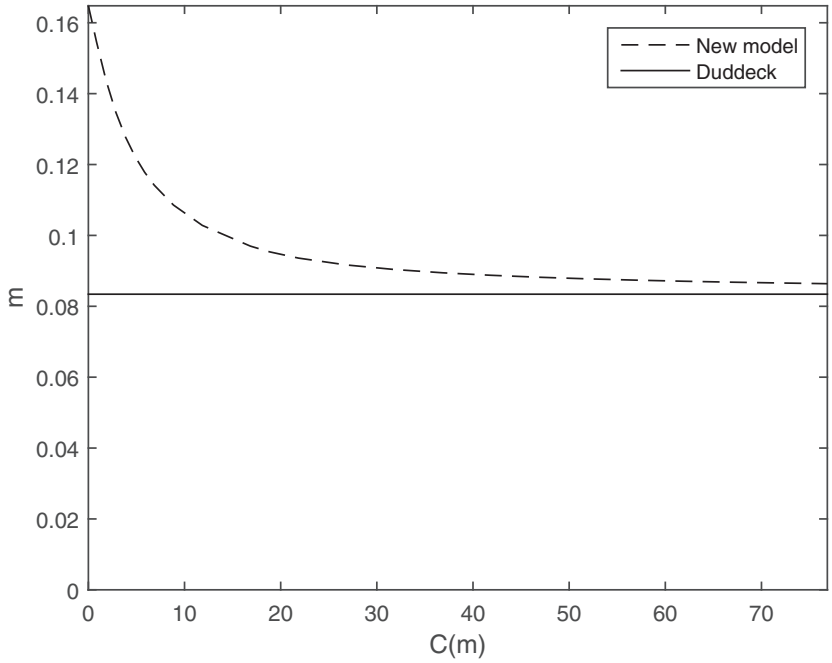

Fig. 8. Normalized maximum bending moments m in models with various values of cover depth C

where σ_v = vertical soil pressure at the tunnel spring line; and m = normalized maximum moment.

Fig. 7 shows a comparison between the normalized maximum moments m derived from the new model and Duddeck's model (Duddeck and Erdmann 1985) in various relative stiffness α_D of soil and the tunnel lining. Overall, the normalized maximum bending moments of the new model show the same trend as Duddeck's model but have greater values. With the greater α_D value corresponding with stiffer ground or more flexible tunnel linings, the normalized maximum moments m derived from the new model are closer to these moments from Duddeck's model.

Fig. 8 shows the changes of the normalized maximum bending moments m derived from these models with the cover depth of the tunnel C. With Duddeck's method (Duddeck and Erdmann 1985), the m value does not change with varied depths of the tunnel (in this case m = 0.083). Meanwhile, the m value in the new model is greater than in Duddeck's model and becomes constant and close to the m value of Duddeck's model when the tunnel is at great depths. In the range of C from 0 to 12.6 m or C/D from 0 to 2 in the case of shallow tunnels, the m value in the new model is much higher than the m value in Duddeck's model. Especially for tunnels close to the surface

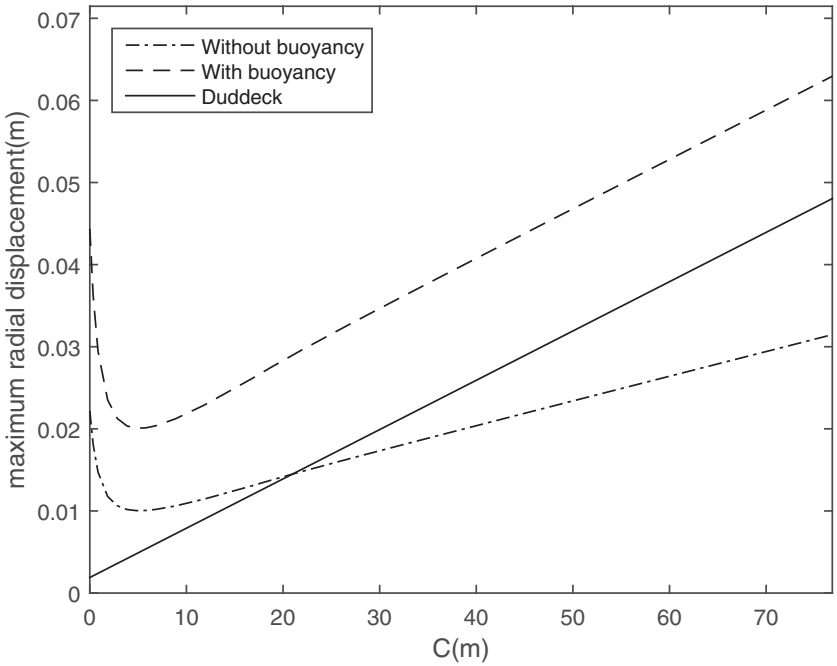

Fig. 9. Maximum radial displacements in models with varied values of cover depth C

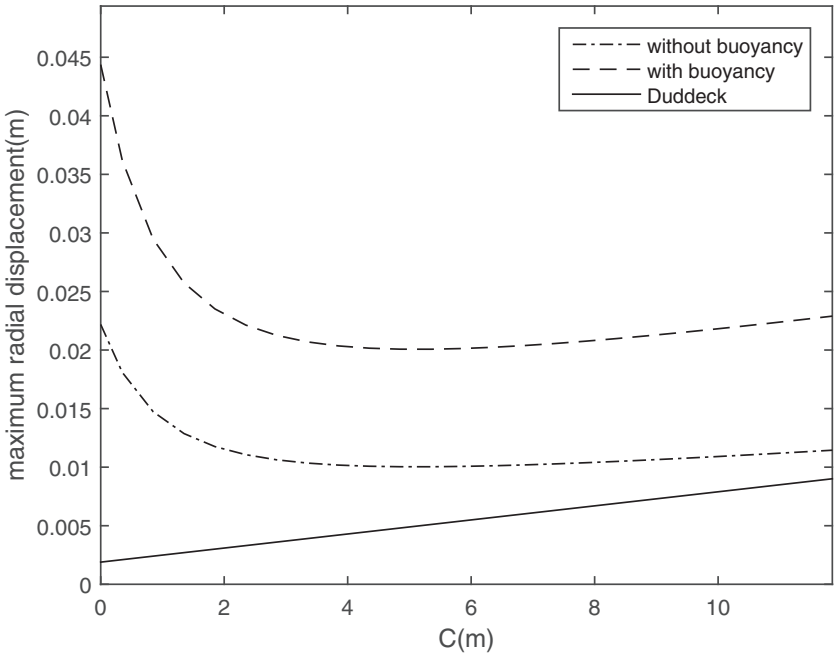

Fig. 10. Maximum radial displacements in models in shallow tunnels

(the cover depth $C \approx 0$ m), the m value in the new model is double that in Duddeck's model. This stems from the previously mentioned analysis of the loading in the tunnel lining models. In Duddeck's model, the loading on the tunnel lining is assumed as symmetric loading in both vertical and horizontal axes of the tunnel. This leads to the maximum bending moments appearing at the top and at the bottom of the tunnel cross section and having the same value. In the new model, the loading on the tunnel lining changes with the depth of a particular point of the tunnel cross section. Consequently, the bending moments at the top and at the bottom of the tunnel cross section are different. In shallow tunnels, the loading at the bottom of the tunnel lining is significantly greater than the overburden loadings at the top and at the spring line of the tunnel lining. Therefore, the normalized maximum bending moment m in the new model is much greater than in Duddeck's model in the case of shallow tunnels, which also means that the maximum bending moment calculated from the new model is significantly greater than the maximum bending moment calculated from Duddeck's model. The larger bending moment generates greater deformations of the tunnel lining; thus, there are larger soil movements around the tunnel lining. These large soil

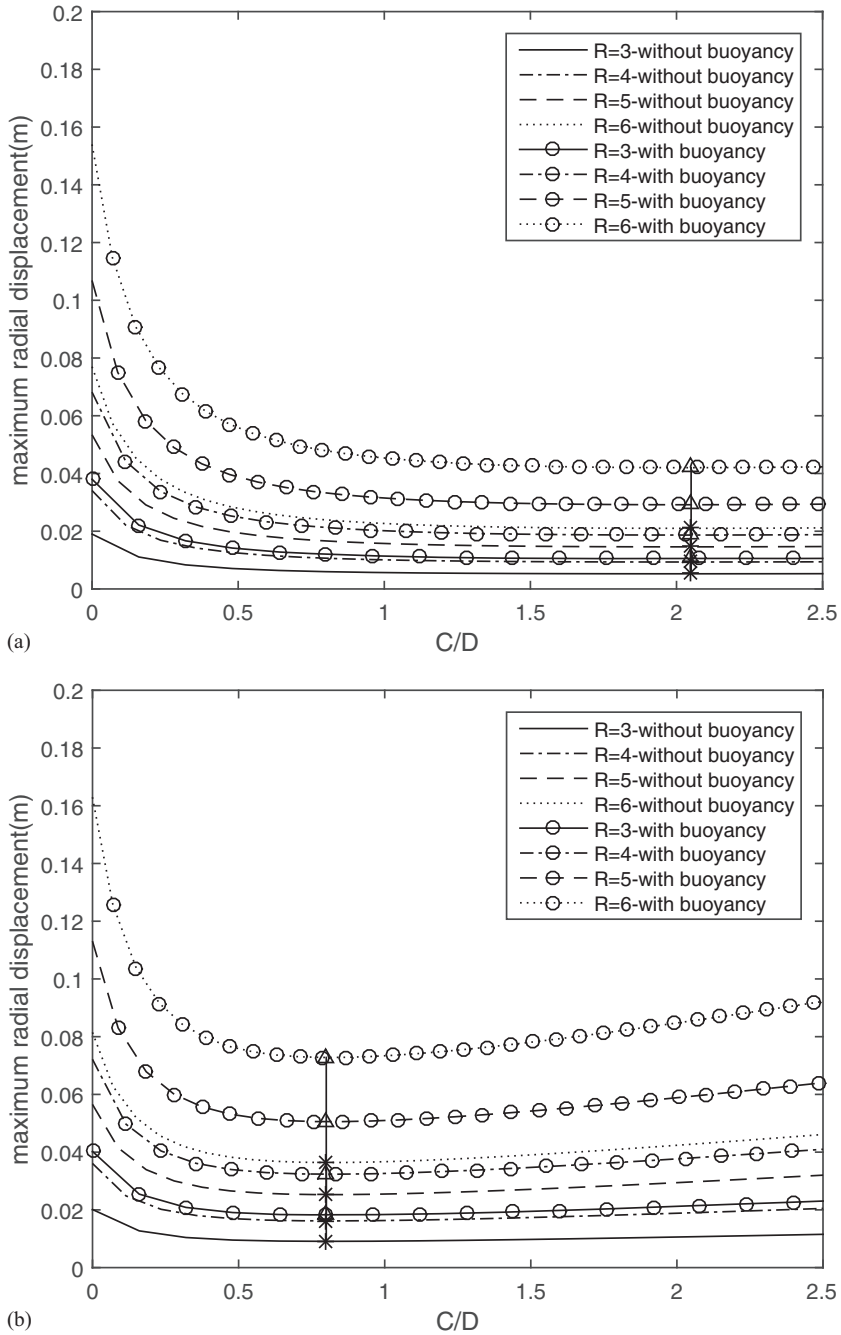

Fig. 11. Relationship between maximum radial displacements and cover-to-diameter C/D values for models with and without buoyancy in varied thickness-to-diameter ratios d/D of the tunnel cross section (vertical lines include the optimal C/D, in which radial displacement is minimal): (a) $d/D = 1/10$; (b) $d/D = 1/20$; (c) $d/D = 1/40$

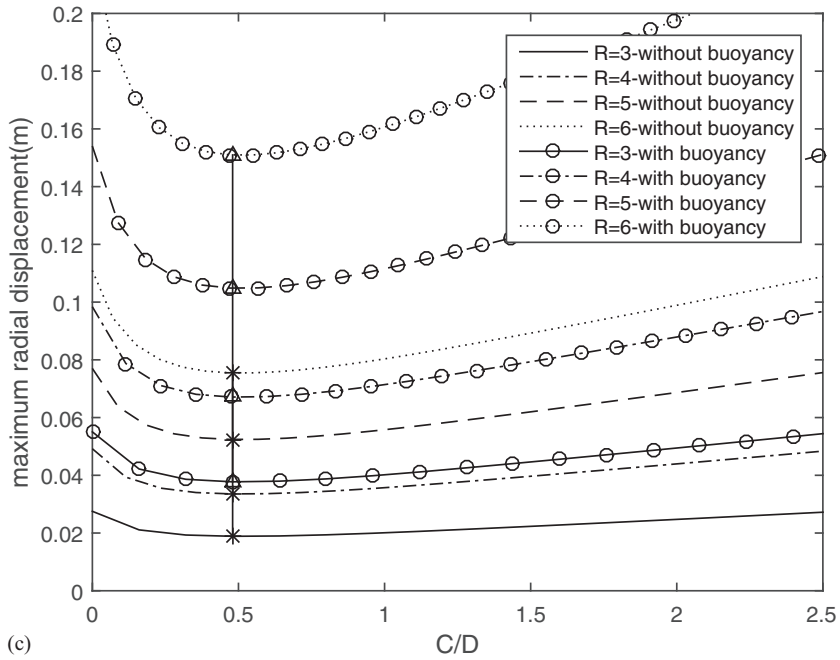

Fig. 11. (*Continued.*)

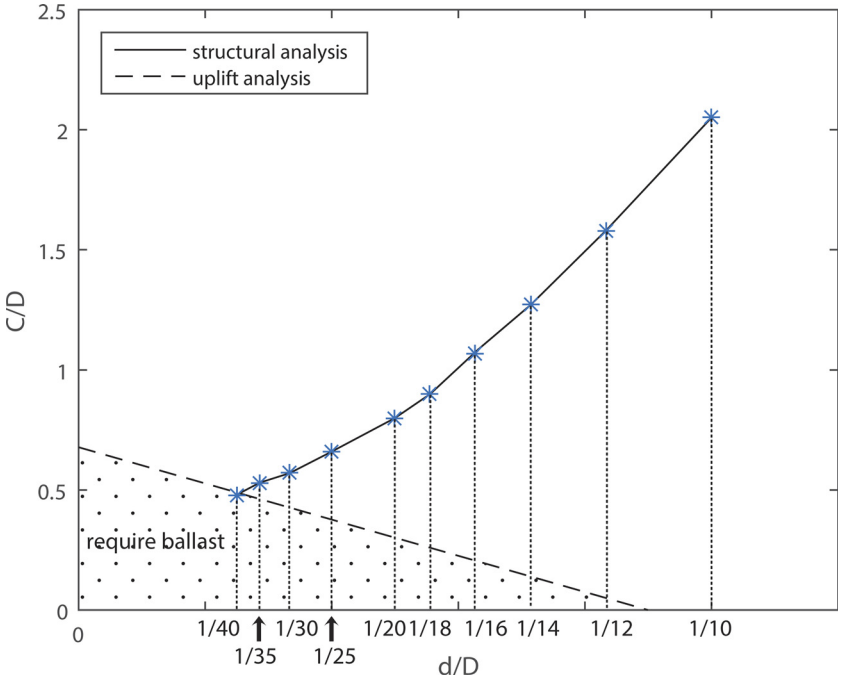

Fig. 12. Optimal cover-to-diameter ratio C/D values for shallow tunnels (for soil with $K = 0.5$, $\nu = 0.2$, $\gamma = 20\,\text{kN/m}^3$, and $E = 20{,}000\,\text{kN/m}^2$)

movements can influence the spring stiffness. However, this impact is not taken into account in this study because the ground is assumed as an elastic material, as indicated in the previous assumptions, and the springs are linear elastic. When the tunnel is at greater depths, the loading in the new model converges to the loading in Duddeck's model, even though a small difference between the loadings at the top and at the bottom of the tunnel lining remains. The normalized maximum bending moment m in the new model, therefore, becomes nearly equal to the m value in Duddeck's model in this case.

One of the most important considerations in tunnel design is the deformation of the tunnel lining. Figs. 9 and 10 show the changes of maximum radial displacements in these models at various depths of the tunnel. In Fig. 9, in the analysis results obtained from Duddeck's model (Duddeck and Erdmann 1985), the maximum radial displacement of the tunnel lining increases linearly with an increase in tunnel depth. When the tunnel is located below the water level, there is an upward force equal to the displaced volume of water. This phenomenon is known as buoyancy. This trend also appears in the new

model with and without buoyancy for moderate and deep tunnels ($C \geq 6.3$m or $C/D \geq 2$). Maximum radial displacement in the new model with buoyancy is higher than that in Duddeck's model due to the higher maximum bending moments, as indicated in the previously mentioned analysis.

Fig. 10 shows the change in the maximum radial displacement in the case of shallow tunnels ($C/D \leq 2$). Maximum radial displacements in the new model with and without buoyancy are higher than the maximum radial displacement in Duddeck's model (Duddeck and Erdmann 1985). In the analysis results from Duddeck's model, the maximum radial displacement decreases linearly to nearly 0 when the tunnel is close to the surface. Clearly, this is not appropriate for practical cases. Therefore, it might be risky when applying Duddeck's model in designing very shallow tunnels. For very shallow tunnels (C/D from 0 to 1 or C from 0 to 6.3 m in this paper), the maximum radial displacement increases sharply in the buoyancy model and significantly in the model without buoyancy when the tunnel is near the surface. If one compares the two, then the maximum radial displacements in the buoyancy model are two to three times higher than displacements in the model without buoyancy. This happens when the tunnel is close to the surface because the relative difference in the loading on the upper and lower parts of the tunnel lining increases more both for soil loading and pore pressure.

From the maximum radial displacement lines of the new model given in Fig. 10, there are lowest points with and without buoyancy. This indicates the existence of an optimal depth for a particular tunnel in which maximum deformation is minimal both with and without buoyancy. In this case study, the optimal depth is estimated at the depth of the tunnel $H = 8.5$ m or the cover depth $C = 5.35$ m, in which the minimum values of maximum displacements in models with and without buoyancy are 0.02 and 0.01 m, respectively.

Analyzing for varied tunnel radii R and the thickness-to-diameter d/D ratio of cross sections in the new model with and without buoyancy, Fig. 11 shows the relationship between maximum radial displacements and the C/D ratio. At a particular value of the C/D ratio, the thinner the tunnel cross section and/or the larger the tunnel radius is, the larger is the maximum radial displacement. It is interesting to note the existence of a value of the C/D ratio in which the maximum radial displacement is minimum for a particular d/D ratio with varied tunnel radii R both with and without buoyancy. In Fig. 11(a) for the tunnel with cross section $d/D = 1/10$, the maximum displacement of the tunnel lining reaches the minimum value when $C/D = 2.05$ for the models with and without buoyancy. These optimal values are 0.8 for the tunnel with cross section $d/D = 1/20$ in Fig. 11(b) and 0.48 for the tunnel with cross section $d/D = 1/40$ in Fig. 11(c).

On the basis of this structural analysis for shallow tunnels in soft soil, for a varied geometry of the cross section of the tunnel d/D, an optimal C/D value can be found that gives a minimum value of the maximum deformation of the tunnel lining. Moreover, uplift analysis for shallow tunnels in Vu et al. (2015) provides the minimum C/D ratio in which ballast should be used for varied values of d/D. From Fig. 12, the optimal C/D value based on the structural analysis and uplift analysis for shallow tunnels with or without buoyancy can be determined. The intersection between the optimal values of the C/D ratio from structural analysis and uplift analysis shows a designed shallow tunnel in which ballast layers are required or in which the value of the d/D ratio should be minimally used in a particular depth of the tunnel.

Conclusions

Structural design for tunnels has been previously focused on moderate to deep tunnels ($C/D \geq 2$). The loading on tunnel linings in recent models does not include the difference of loadings at the top and at the bottom of shallow tunnels. By calculating the soil pressure at particular points on the cross section of the tunnel combined with the FEM for structural analysis, the new model in this study becomes appropriate for tunnels at shallow depths. Structural analysis from the new model shows that the normalized internal forces and the deformations of the tunnel lining increase significantly when the tunnel is designed at shallow location with and without buoyancy. From the analysis results it follows that there is a minimum value of maximum deformation of the tunnel lining when changing the cover depth C of the tunnel. From combined structural analysis with uplift analysis, an optimal cover-to-diameter ratio C/D value for a particular cross section d/D value in tunneling without ballast can be derived.

References

ANSYS [Computer software]. ANSYS, Canonsburg, PA.

Ahrens, H., Lindner, E., Lux, K. H. (1982). "Zur dimensionierung von tunnelausbauten nach empfehlungen zur berechnung von tunneln im lockergestein, 1980." *Bautechnik*, 59(8), 260–273.

Bakker, K. (2003). "Structural design of linings for bored tunnels in soft ground." *Heron*, 48(1), 33–64.

Bakker, K., Leendertse, W., Jovanovic, R., and van Oosterhout, G. (2000). "Monitoring: Evaluation of stresses in the lining of the Second Heinenoord Tunnel." *Geotechnical aspects of underground construction in soft ground*, A. A. Balkema, Tokyo, 197–202.

Bakker, K. J. (2000). *Soil retaining structures: Development of models for structural analysis*, A. A. Balkema, Rotterdam, Netherlands.

Blom, C. B. M. (2002). "Design philosophy of concrete linings for tunnels in soft soils." Ph.D. thesis, TU Delft, Delft Univ. of Technology, Delft, Netherlands.

Broere, W. (2001). "Tunnel face stability & new CPT applications." Doctoral thesis, TU Delft, Delft Univ. of Technology, Delft, Netherlands.

Do, N. A., Dias, D., Oreste, P., and Djeran-Maigre, I. (2014). "A new numerical approach to the hyperstatic reaction method for segmental tunnel linings." *Int. J. Numer. Anal. Methods Geomech.*, 38(15), 1617–1632.

Duddeck, H. (1988). "Guidelines for the design of tunnels." *Tunnelling Underground Space Technol.*, 3(3), 237–249.

Duddeck, H., and Erdmann, J. (1985). "On structural design models for tunnels in soft soil." *Underground space*, Vol. 9, Pergamon Press, Oxford, U.K., 246–259.

Einstein, H. H., and Schwartz, C. W. (1979). "Simplified analysis for tunnel supports." *J. Geotech. Eng. Div., Am. Soc. Civ. Eng.*, 105(4), 499–518.a66.

Groeneweg, T. (2007). "Shield driven tunnels in ultra high strength concrete: Reduction of the tunnel lining thickness." M.Sc. thesis, TU Delft, Delft Univ. of Technology, Delft, Netherlands.

Mashimo, H., and Ishimura, T. (2005). "Numerical modelling of the behavior of shield tunnel lining during assembly of a tunnel ring." *Proc., 5th Int. Symp. Geotechnical Aspects of Underground Construction in Soft Ground*, Taylor & Francis, Amsterdam, Netherlands, 587–593.

Molins, C., and Arnau, O. (2011). "Experimental and analytical study of the structural response of segmental tunnel linings based on an in situ loading test. Part 1: Test configuration and execution." *Tunnelling Underground Space Technol.*, 26(6), 764–777.

Möller, S. C. (2006). "Tunnel induced settlements and structural forces in linings." Ph.D. thesis, Univ. Stuttgart, Inst. f. Geotechnik, Stuttgart, Germany.

Morgan, H. (1961). "A contribution to the analysis of stress in a circular tunnel." *Géotechnique*, 11(1), 37–46.

Muir Wood, A. M. (1975). "The circular tunnel in elastic ground." *Géotechnique*, 25(1), 115–127.

Muir Wood, A. M. (1976). "Discussion: The circular tunnel in elastic ground." *Géotechnique*, 26(1), 231–237.
Oreste, P. (2007). "A numerical approach to the hyperstatic reaction method for the dimensioning of tunnel supports." *Tunnelling Underground Space Technol.*, 22(2), 185–205.
PLAXIS [Computer software]. PLAXIS, Delft, Netherlands.
Plizzari, G., and Tiberti, G. (2006). "Steel fibers as reinforcement for precast tunnel segments." *Tunnelling Underground Space Technol.*, 21(3), 438–439.
Schmid, H. (1926). *Statische probleme des tunnel-und druckstollenbaues und ihre gegenseitigen beziehungen*, Springer, Berlin.
Schulze, H., and Duddeck, H. (1964). "Spannungen in schildvorgetriebenen tunneln." *Beton-und Stahlbetonbau*, 59(8), 169–175.
Vu, M. N., Broere, W., and Bosch, J. W. (2015). "The impact of shallow cover on stability when tunnelling in soft soils." *Tunnelling Underground Space Technol.*, 50, 507–515.
Windels, R. (1966). "Spannungstheorie zweiter ordnung für den teilweise gebetteten kreisring." *Die Bautechnik*, 43, 265–274.
Windels, R. (1967). "Kreisring im elastischen continuum." *Der Bauingenieur Bd*, 42, 429.
Winkler, E. (1867). *Theory of elasticity and strength*, Dominicus Prague, Prague, Czech Republic.